Journal of Applied Polymer Science

Semi-aromatic polyimide/Ag nanocomposite derived from vanillin

Zeinab Mirzakhanian,[1] Khalil Faghihi,[1] Hossein Ardeshir Geravi,[1] Majid Mahdieh[2]
[1]Department of Chemistry, Faculty of Science, Arak University, Arak 38156-8-8349, Iran
[2]Department of Biology, Faculty of Science, Arak University, Arak 38156-8-8349, Iran
Correspondence to: K. Faghihi (E-mail: khfaghihi@gmail.com)

ABSTRACT: The development of bioprecursor polyimide/Ag nanocomposites (PI/Ag NCs) is reported in this investigation. Semiaromatic bioprecursor PI was successfully synthesized through direct polycondensation reaction between aromatic diamine containing pyridine ring and aliphatic dianhydride. Aromatic diamine as a monomer was synthesized using a renewable resource, vanillin. The main attractive aspects of this PI are the renewable origin of the diamine, presence of pyridine and high aromatic rings content, as well as aliphatic content on the polymer backbone. The structure of synthesized monomer and PI were proven by FTIR, and nuclear magnetic resonance. The PI/Ag NCs containing 3, 5, and 7 wt % of Ag nanoparticles (Ag NPs) were prepared through solution technique and the resulting NCs were characterized by Fourier transform infrared spectra, wide angle X-ray diffraction, transmission electron microscopy (TEM), and thermogravimetric analysis (TGA). TEM results showed that the Ag NPs were dispersed homogeneously in the PI matrix on nanoscale. TGA results indicated improving in thermal properties of PI/Ag NCs compared to the neat PI due to the interaction between the PI matrix and the Ag NPs. Antibacterial activity of PI/Ag NCs was tested by the disk diffusion method using *Escherichia coli* as model strain of gram-negative bacteria. © 2016 Wiley Periodicals, Inc. J. Appl. Polym. Sci. **2016**, *133*, 44001.

KEYWORDS: biopolymers and renewable polymers; composites; polyimides

Received 20 December 2015; accepted 1 June 2016
DOI: 10.1002/app.44001

INTRODUCTION

Over the last decade, the development of polymer metal nanocomposites (NCs) has received rising attention owing to their broad range of potential applications compared with those of neat polymer.[1,2] Among different NPs, silver nanoparticles are widely used due to their superior optical,[3] electrical, catalytic,[4] and antimicrobial properties.[5–7]

Polymer/silver nanoparticles composites, combining the advantages of the silver nanoparticles and the processability of the polymers, have opened a new gateway in developing NC systems with improved performances.[8]

Among many engineering polymers, aromatic polyimides (PIs) are well known as high performance polymers owing to their excellent combination properties, such as high thermal stability, good mechanical property, low dielectric constant, and excellent chemical resistance.[9–12] Due to their properties, such engineering polymers are potential matrices for NCs.

Semiaromatic PIs in particular are of special interest because the limiting factors for processing and application of aromatic PIs, for example, poor solubility in common organic solvents and extremely high transition temperatures, have been improved for them.[13–15]

However, most of the PIs are prepared with petroleum-based monomers as the raw materials. The dwindling fossil fuels and the growing environmental concerns have motivated developments of polymers from biorenewable raw materials.[16] The development of green monomers/polymers from easily renewable feed stocks therefore has gained considerable interest in the past few years.[17,18] In polymer science, a large number of polymers are based on aromatic monomers, while very few molecular aromatic compounds from renewable resources are readily available. Consequently, there were only a few reports dealing with the preparation of PIs from bio-based monomers.

Vanillin, a naturally occurring phenol, is one of the aromatic compounds from renewable resources that is currently one of the only bio-based and aromatic compounds that is industrially available. Vanillin has been explored in recent years for synthesis of bio-based monomers and polymers.[19–22]

To obtain bio-based PIs with adequate thermal resistance, monomers with intrinsic rigidity are required. Incorporating of pyridine and its derivatives has been already reported to improve thermal stability of the polymeric matrices.[23–26] The rigid heteroaromatic pyridine ring develops thermal and chemical stability of polymers, while the polarizability of nitrogen atom can improve the solubility in organic solvents.[27,28]

The present study deals with the synthesis and characterization of new semi aromatic bioprecursor PI derived from renewable resource, vanillin, and its subsequent NCs with different amounts of Ag NPs (3, 5, and 7 wt %). The structure of synthesized bioprecursor monomer and PI were proven by Fourier transform infrared spectra (FT-IR), and nuclear magnetic resonance (^{1}H NMR).

The obtained NCs were characterized by FT-IR, UV–Visible spectroscopy, X-ray diffraction (XRD), transmission electron microscopy (TEM), and thermogravimetric analysis (TGA).

Antibacterial activity of PI/Ag NCs was also tested by the disk diffusion method using *Escherichia coli* as model strain of gram-negative bacteria. The main objectives of this research are the preparation of novel bioprecursor PI and investigation the effect of Ag NPs on PI matrix.

EXPERIMENTAL

Materials

Vanillin (4-hydroxy-3-methoxybenzaldehyde), 4-nitroacetophenone, ammonium acetate, and epiclon [5-(2,5-dioxotetrahydro-3-furanyl)−3-methyl-3-cyclohexene-1,2-dicarboxylic anhydride] were purchased from Merck Company (Germany) and used without further purification. Glacial acetic acid, palladium charcoal, hydrazine hydrate, *N*,*N*-dimethylformamide (DMF), ethanol, and *N*,*N*-dimethylacetamide (DMAc) obtained from Aldrich (Milwaukee) were used without further purification. Nanosized Ag powder was purchased from Nanosabz Co. (Tehran, Iran) with an average particle size of 25–35 nm.

Monomer Synthesis

4-(4-hydroxy-3-methoxyphenyl)−2, 6-Bis(4-nitrophenyl)Pyridine. In a 250-mL round-bottom flask, a mixture of 5.0 g (32.9 mmol) of vanillin, 10.85 g (65.8 mmol) of 4-nitroacetophenone, 76.5 g (1.0 mol) of ammonium acetate, and 150 mL of glacial acetic acid was refluxed for 24 h. Upon cooling, the precipitated yellow solid was collected by filtration and washed with ethanol. The yield of the crude product was 64%. Other specifications include m.p.: 275 °C; FT-IR (KBr): 3531 (s), 1593 (s), 1514 (s), 1438 (m), 1346 (s), 1271 (m), 1209 (m), 1103 (m), 1031 (m), 846 (s), and 761 (m) cm^{-1}. ^{1}H NMR (DMSO-d$_6$, TMS) δ: 9.55 (s, 1H), 8.6 (d, 4H), 8.4 (6H), 7.6 (2H), 6.9 (d, 1H), and 3.9 (s, 3H) ppm.

4-(4-hydroxy-3-methoxyphenyl)−2, 6-Bis(4-aminophenyl) Pyridine. In a 250-mL round-bottom flask equipped with a reflux condenser and a dropping funnel, a suspension of the synthesized dinitro (5 g, 12 mmol) and palladium on carbon 10% (0.15 g) in a mixture of ethanol (40 mL) and DMF (5 mL) was prepared. While heated to 80 °C and being stirred magnetically, a solution of hydrazine monohydrate 80% (10 mL) in ethanol (15 mL) was added drop wise through the dropping funnel over a 1-h period. After 4 h, the mixture was filtered, while hot to remove Pd/C, and then the solvent was evaporated under vacuum to afford the yellow solid product. Yield: 84%; m.p.: 215 °C; FT-IR (KBr): 3435 (w), 3330 (m), 3321 (m), 3217 (m), 1658 (w), 1597 (s), 1543 (m), 1512 (s), 1392 (m), 1267 (m), 1178 (m), 1124 (m), 1026 (w), 829 (m), 752 (m), and 580 (m) cm^{-1}. ^{1}H NMR (DMSO-d$_6$, TMS) δ: 9.3 (s, 1H), 7.9 (d, 4H), 7.7 (2H), 7.4 (d, 1H), 7.3 (m, 1H), 6.9 (d, 1H), 6.6 (d, 4H), 5.3 (s, 4H), and 3.9 (s, 3H) ppm.

Synthesis of Bioprecursor PI

A typical procedure to prepare PI by thermal imidization was used as follows: equimolar amount of synthesized diamine and dianhydrid (epiclon) was dissolved in DMAc stirring at room temperature for 24 h under N_2 atmosphere to form polyamic acid (PAA). The resulting PAA solution was cast on to a glass and placed in an oven for a programmed heat treatment: 1 h at 80 °C, 1 h at 120 °C, 1 h at 160 °C, and 4 h at 200 °C.

Preparation of Bioprecursor PI/Ag NCs

For the preparation of PI/Ag NCs, equimolar amount of diamine and dianhydrid (epiclon) was dissolved in DMAc stirring at room temperature for 24 h under N_2 atmosphere to form PAA. Then, different amounts of Ag NPs (3, 5, and 7 wt % of PI) were mixed with the PAA solution by stirring for another 2 h at room temperature and sonicating for 30 min. By casting the resulting mixtures on to a clean glass petri dishes and then step curing (at each temperature of 80, 120, and 160 °C for 1 h and 200 °C for 4 h, respectively), the PI/Ag NCs were obtained.

Characterization

FT-IR data were recorded on Galaxy series FTIR 5000 spectrophotometer (England). Vibration transition frequencies were reported in wave number (cm^{-1}). Band intensities were assigned as weak (w), medium (m), shoulder (sh), strong (s), and broad (br). For sample preparation, the powdered species were mixed with KBr and pressed in form of pellets and used for further characterization.

^{1}H NMR measurements were performed using Bruker Avance 400 spectrometer. DMSO-d$_6$ was used as the solvent, and the solvent signal was used for internal calibration (DMSO-d$_6$: δ (^{1}H) = 2.5 ppm). UV–Visible spectrum was recorded at room temperature in 250–600 nm spectral regions using Optizen 3220 UV–Visible spectrophotometer. Wide angle X-ray diffraction patterns were recorded using a Philips X'Pert PW 3373 diffractometer (Cu K radiation, λ = 1.54056 Å, 40 kV, 40 mA) scanning from 2 to 80 °C at 2 °C min^{-1}.

The morphological analysis was carried out using TEM with Zeiss-EM10C microscope. For preparing TEM samples, DMAc-sonicated solution of samples was dropped directly into copper grids (lacey carbon coated grid Cu Mesh 300) and after drying was analyzed.

Thermal stability of polymer and NCs was measured by TGA (TA instruments Perkin-Elmer 4000) in the range between room temperature and 900 °C at a heating rate of 10 °C min^{-1} in nitrogen atmosphere.

Antibacterial Assessments

Antibacterial activity of PI and PI/Ag NCs was tested by disk-diffusion method also known as the Kirby–Bauer method according to the guidelines set by the National Committee for Clinical and Laboratory Standards (now renamed as Clinical and Laboratory Standards Institute, 2000).

E. coli as an example of gram-negative bacteria was used as target organism. All disks and materials were sterilized in an autoclave before the experiment, and all antibacterial tests were

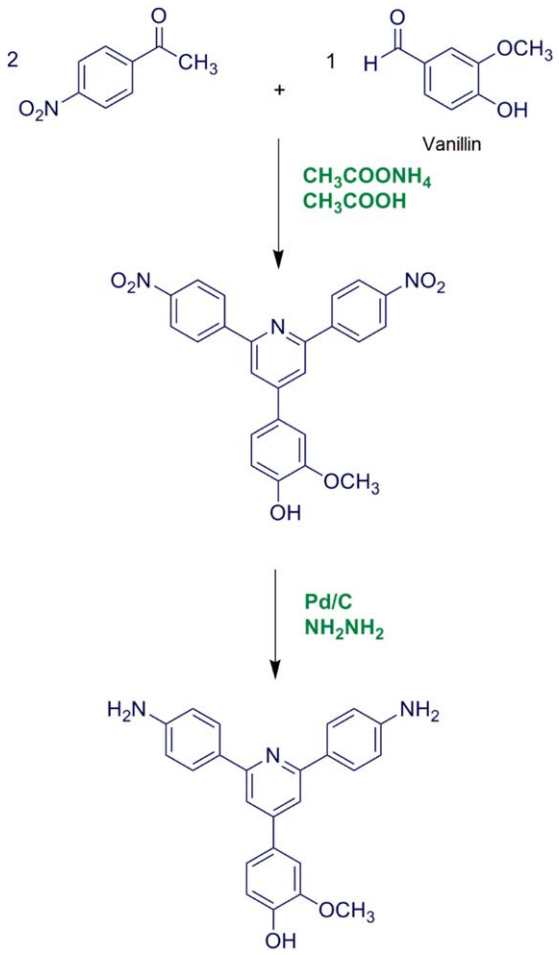

Scheme 1. Synthesis route of the bio-based diamine from vanillin. [Color figure can be viewed in the online issue, which is available at wileyonlinelibrary.com.]

carried out in triplicate. Muller–Hinton (MH) agar medium was prepared and sterilized in an autoclave. *E. coli* was grown in sterile MH culture medium at 37 °C overnight.

The agar medium was poured into the sterile Petri plates when the medium was in a warm molten state. After the medium solidified, liquid culture with bacteria (*E. coli*) was spread onto sterile petri plates with cotton swabs. Blank disks (6 mm diameter) were saturated by adding 40 μL of samples solution (20 mg/mL in DMSO) and were placed on the center of each petri plate and pressed gently. After incubating at 37 °C for 24 h, the zone of inhibition around each sample was measured. The average diameter of the inhibition zones (mm) produced by the samples was used to express antibacterial activity. All antibacterial tests were carried out in triplicate.

RESULTS AND DISCUSSIONS

Monomer Synthesis

Vanillin, a naturally occurring phenol, was used for the synthesis of bio-based diamine. Chichibabin method[29] was used for the preparation of dinitro compound containing pyridine ring (Scheme 1).[30–34] In particular, the condensation of renewable vanillin, along with 4-nitroacetophenone in the presence of ammonium acetate afforded the dinitro compound in one step. Later, diamine was synthesized by using dinitro and hydrazine hydrate as the source of hydrogen and palladium on charcoal (10%) as the catalyst in a reduction reaction.

The structure of synthesized diamine was confirmed by ^{1}H NMR. The ^{1}H NMR spectrum of the diamine showed the characteristic resonance of two amine groups at 5.3 ppm and phenolic O–H at 9.3 ppm. The CH_3 proton was evident at 3.9 ppm, while the aromatic protons appeared in the region of 6.6–8.0 ppm (Figure 1).

Synthesis of Bio-Precursor PI

The semiaromatic bioprecursor PI was synthesized via direct polycondensation reaction of an equimolar mixture of aliphatic dianhydride (epiclon) with the heterocyclic aromatic diamine (Scheme 2). Introduction of aliphatic dianhydride units and bulky aromatic pendant groups in the polymer backbone is a successful approach to improve processability of PIs. Moreover, the rigid-aromatic pyridine ring develops thermal and chemical

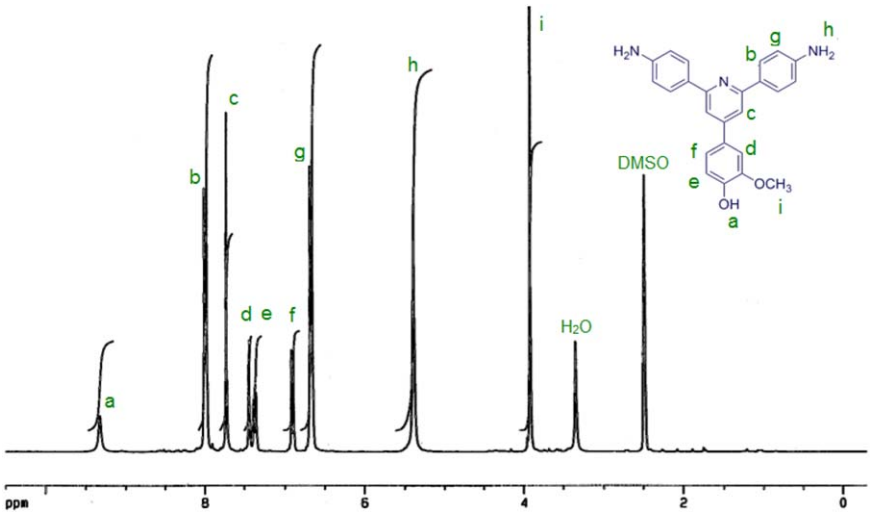

Figure 1. ^{1}H NMR spectrum of the bio-based diamine in DMSO-d_6. [Color figure can be viewed in the online issue, which is available at wileyonlinelibrary.com.]

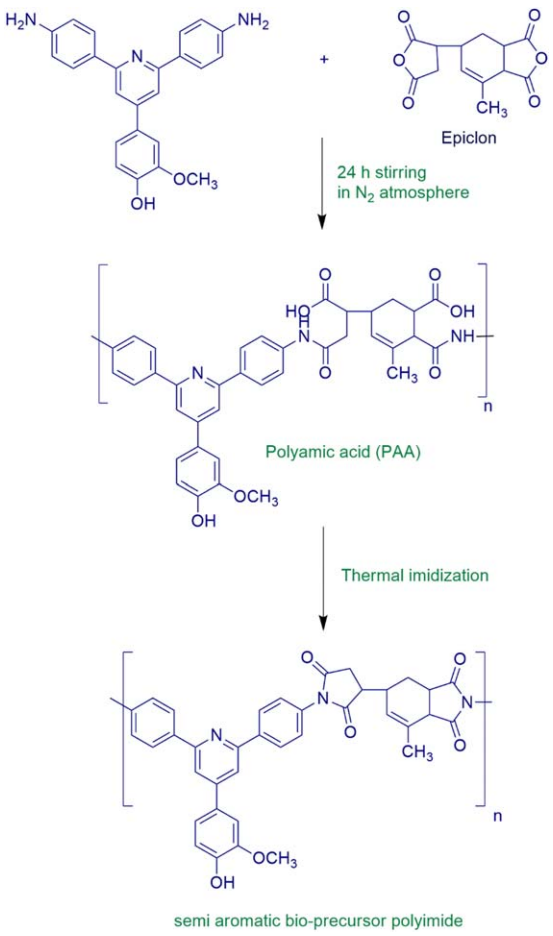

Scheme 2. Synthesis route of semi aromatic bio-precursor PI. [Color figure can be viewed in the online issue, which is available at wileyonlinelibrary.com.]

stability of polymer, while the polarizability of nitrogen atom can improve the solubility in organic solvent.[35]

The solubility of PI was investigated using 0.01 g of PI sample in 2 mL of solvent. Due to the presence of bulky pendent groups and flexible aliphatic units, PI had good solubility in organic solvent. Synthesized PI was soluble in polar organic solvents such as dimethyl sulfoxide (DMSO), DMF, DMAc, and *N*-methyl-2-pyrrolidone at room temperature and was insoluble in solvents such as methanol, ethanol, and water.

^{1}H NMR analysis of the synthesized PI confirmed the successful polymer formation. As we can see in ^{1}H NMR spectrum of PI (Figure 2), the proton of the O–H group appeared at 9.4 ppm. The resonance of aromatic and aliphatic protons appeared in the range of 6.9–8.2 and 1.9–3.9 ppm, respectively. The resonance of olefinic protons corresponding to epiclon appeared in 5.6 ppm.

Preparation of Bioprecursor PI/Ag NCs

Novel bioprecursor PI/Ag NCs containing 3, 5, and 7 wt % of Ag NPs were successfully prepared in dry DMAc through solution technique. The reaction pathway for the preparing of PI/Ag NCs is shown in Scheme 3.

The presence of pyridine ring, hydroxyl, and methoxy groups in chain of polymer performs interaction with Ag NPs that can improve physical and morphological properties of the resulting NCs. The possible interactions between PI chains and Ag NPs are shown in Scheme 3.

Characterization of the NCs

FT-IR Study. The FT-IR spectra of neat PI and PI/Ag NCs (3, 5, and 7 wt % of Ag NPs) are shown in Figure 3. In the FT-IR spectrum of PI, the absorption bands at 1709 and 1770 cm^{-1} for the imide ring (symmetric and asymmetric C═O stretching vibration), 1371 cm^{-1} for C–N stretching, and 754 cm^{-1} for C═O bending confirmed the imide formation. The O–H stretching vibrations, centered at 3410 cm^{-1} is due to hydroxyl moieties in the phenolic groups of diamine, and the bands at 2854 and 2930 cm^{-1} are attributed to the symmetric and asymmetric vibrations of methane, respectively.

FT-IR spectrum of PI/Ag NCs exhibited all characteristic absorption peaks corresponding to the PI. It is noteworthy to mention that the relative intensity of the peaks in the PI/Ag NCs is lower than in the pure PI, probably due to the presence of Ag NPs in the PI/Ag NCs.

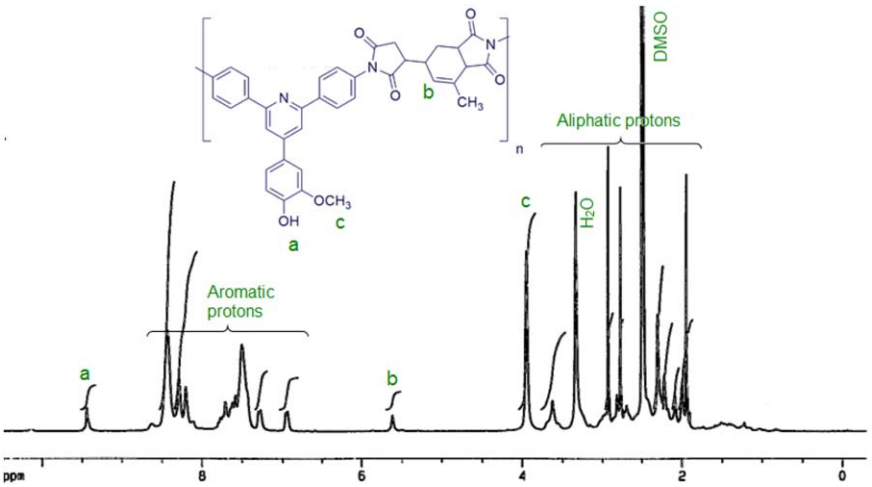

Figure 2. ^{1}H NMR spectrum of PI in DMSO-d_6. [Color figure can be viewed in the online issue, which is available at wileyonlinelibrary.com.]

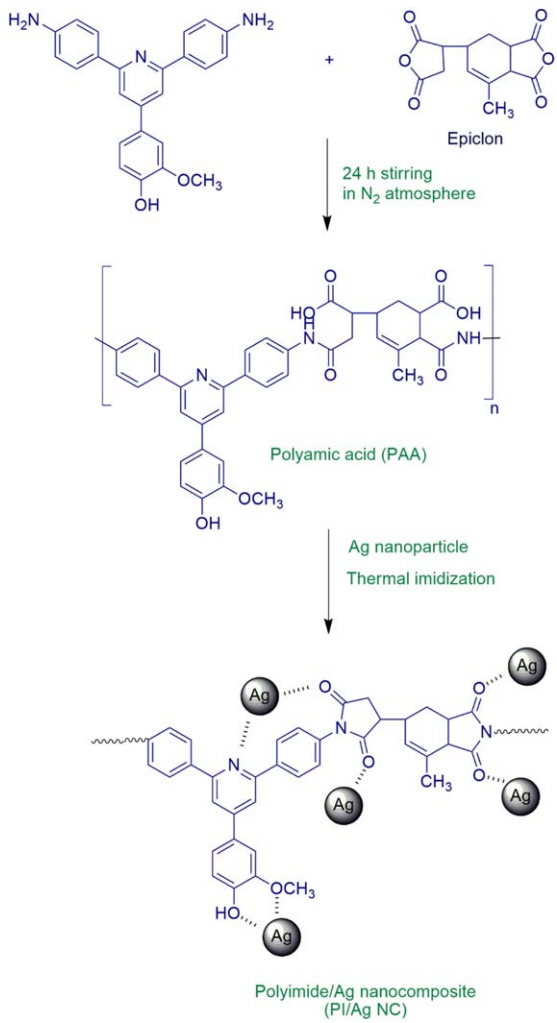

Scheme 3. Synthesis route of PI/Ag NCs. [Color figure can be viewed in the online issue, which is available at wileyonlinelibrary.com.]

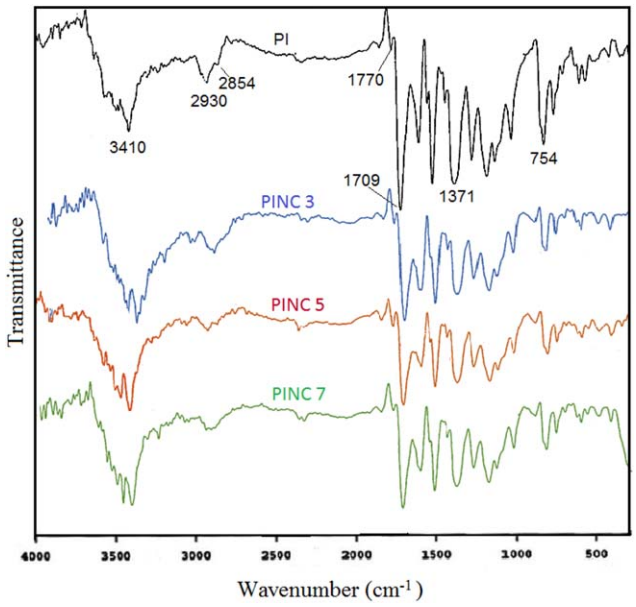

Figure 3. FTIR spectrums of PI and PI/Ag NCs. [Color figure can be viewed in the online issue, which is available at wileyonlinelibrary.com.]

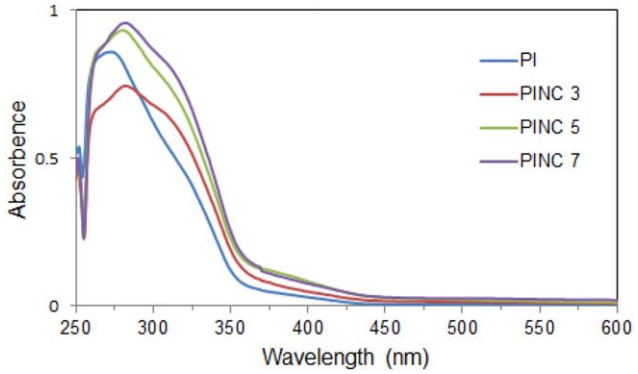

Figure 4. UV–Visible absorption spectra of PI and PI/Ag NCs. [Color figure can be viewed in the online issue, which is available at wileyonlinelibrary.com.]

UV–Visible Absorption Characteristics. The presence of embedded Ag NPs within the PI network was confirmed using UV–Visible spectrophotometry. UV–Visible spectrum of PI and PI/Ag NCs (3, 5, and 7 wt %) is presented in Figure 4.

PI and PI/Ag NCs exhibited strong UV–Visible absorption bands with a maximum absorption (λ_{max}) at 270 and 290 nm, respectively, assignable to π–π^* transition (of the phenyl rings) resulting from the conjugation between the aromatic rings and nitrogen and oxygen atoms.[36,37]

UV spectra of PI/Ag NCs exhibited a characteristic absorption peak near 400 nm, which arises from the surface plasmon absorbance of silver nanoparticles, and its intensity increases with Ag NPs content.

XRD Analysis. Due to its ease of use and availability, XRD is most commonly applied to probe the morphology of the polymer and NCs. The XRD patterns of the virgin PI and PI/Ag NCs (3, 5, and 7 wt %) are presented in Figure 5. The XRD pattern of PI revealed a broad peak at $2\theta = 20°$, which indicated that PI is amorphous.[38]

In the XRD patterns of PI/Ag NCs, four obvious new peaks are detected at $2\theta = 38.1$, 44.3, 64.4, and 77.3°, which are corresponding to the crystal faces of (1 1 1), (2 0 0), (2 2 0), and (3 1 1), respectively, of Ag NPs, consistent with the presence of

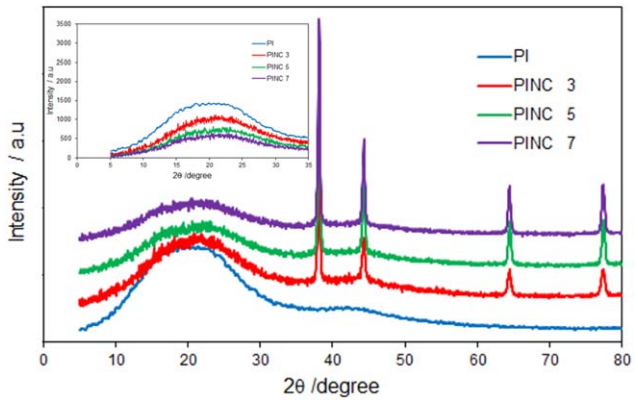

Figure 5. XRD patterns of neat PI and PI/Ag NCs. [Color figure can be viewed in the online issue, which is available at wileyonlinelibrary.com.]

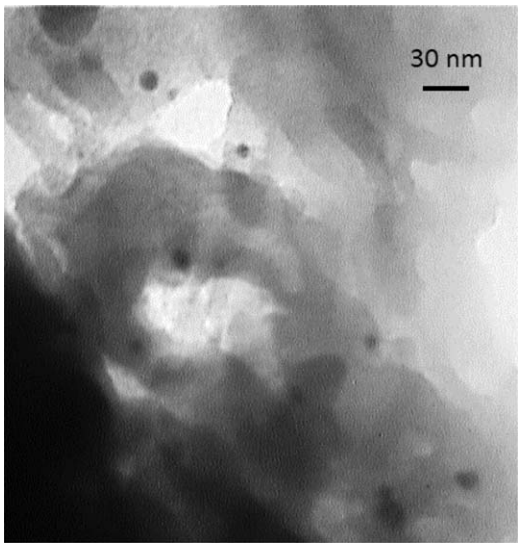

Figure 6. TEM micrograph of PI/Ag NC 3 wt %.

face centered-cubic silver crystallite in the PI. It is also clear that the intensity of these peaks has enhanced with increasing the Ag NPs content.

It is seen in Figure 5, (inset), as the percentage of Ag NPs increases, the peak intensity of PI at $2\theta = 20^{\circ}$ decreases, because the inter crosslinking of the PI chains may be getting weaker. Thus, from these XRD data, it is understood that chemical interactions exist between PI chains and Ag NPs.

Morphology of PI/Ag NCs. The nanoscale dispersion of the Ag NPs within the PI matrix is further corroborated with TEM analysis. The TEM image of the PI/Ag NC containing (3 wt %) Ag NPs is presented in Figure 6. The dark spots indicate the Ag NPs, while the background corresponds to PI matrix.

The TEM image of the PI/Ag NC showed that the silver nanoparticles were homogeneously dispersed in PI matrix, and the average size of the Ag NPs was estimated to be about 25–35 nm. The dispersion of Ag NPs in the PI matrix is due to the good interfacial interactions and chemical compatibility between the PI matrix and Ag NPs.

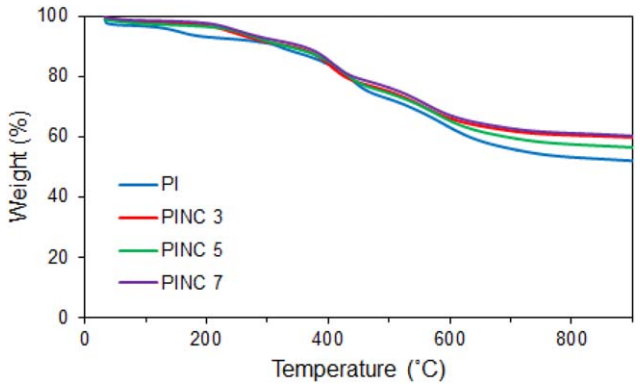

Figure 7. TGA thermograms of PI and PI/Ag NCs. [Color figure can be viewed in the online issue, which is available at wileyonlinelibrary.com.]

Table I. Summarized TGA Analysis Data for PI and PI/Ag NCs

Samples	T_5 (°C)[a]	T_{10} (°C)[b]	Char yield (%)[c]
PI	150	317	51.9
PI/Ag NC 3	237	336	59.7
PI/Ag NC 5	248	331	56.4
PI/Ag NC 7	254	357	60.1

[a] Temperature at which 5% weight loss was recorded by TGA at a heating rate of 10 °C min^{-1}.
[b] Temperature at which 10% weight loss was recorded by TGA at a heating rate of 10 °C min^{-1}.
[c] Weight percentage of material left after TGA analysis at a maximum temperature of 900 °C.

Thermal Properties. Thermal properties of PI and PI/Ag NCs with different Ag NP loadings (3, 5, and 7 wt %) under nitrogen atmosphere were examined by TGA at a heating rate of 10 °C min^{-1}. The consequent weight loss versus operating temperature is plotted in Figure 7. The detailed TGA data, 5% (T_5) and 10% (T_{10}) weight loss temperatures, and char yield for PI and PI/Ag NCs are summarized in Table I. The TGA data indicate that the PI and the NCs possess high thermal stability.

Initial weight loss temperature (T_5) and T_{10} of the NCs are higher than neat PI and have enhanced by increasing Ag NPs content in PI. This enhancement of thermal stability of the NCs can be attributed to the high heat resistance exerted by Ag NPs and strong interactions between Ag NPs and the PI. The results of thermal analysis also show that the residual weight at 900 °C (char yield) has improved by increasing the Ag NPs content.

Comparing the data, it is clear that the PI/Ag NCs 7 shows a significant improvement of T_5 and T_{10} and char yield compared with the PI/Ag NCs 3 and PI/Ag NCs 5. It is clear that uniform dispersion of Ag NPs is very crucial for improvement of the thermal property.[39] The results confirm well dispersion of Ag NPs in PI Ag NCs.

Antibacterial Assessments. The antibacterial activity of pure PI and PI/Ag NCs (3, 5, and 7 wt %) was tested for *E. coli*, using the diameter of inhibition zone (DIZ) in a disk diffusion test. The DIZ reflects the magnitude of susceptibility to microorganisms. The strains susceptible to disinfectants exhibit larger DIZ, whereas resistant strains exhibit smaller DIZ.

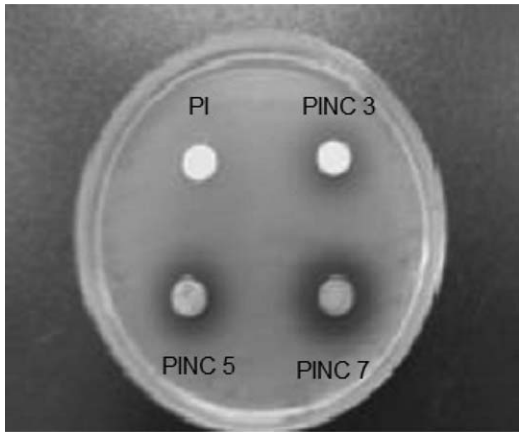

Figure 8. Antibacterial activity of pure PI and PI/Ag NCs.

No zone of inhibition was observed around the PI disk, while the disks of PI/Ag NCs were surrounded by a clear and significantly larger DIZ for *E. coli*. The inhibition zone diameters of PI/Ag NCs (3, 5, and 7) were 8, 11, and 15 mm, respectively, indicating that PI/Ag NCs are effective antibacterial agents. PI/Ag NC 7 showed much better antibacterial activity than others (Figure 8).

CONCLUSIONS

In this investigation, semiaromatic bioprecursor PI was synthesized using vanillin as easily renewable resource. In addition to the renewable origin of PI, introduction of bulky aromatic groups, pyridine, and aliphatic groups is attractive aspect of this PI that increases the flexibility of polymer.

The PI/Ag NCs reinforced with three different amounts of Ag NPs (3, 5, and 7 wt %) were prepared through solution technique and characterized by FT-IR, UV–Visible, and XRD. The results showed chemical interaction between PI chains and Ag NPs. TEM results have also revealed homogenous dispersion of Ag NPs within the PI matrix.

The addition of Ag NPs into a PI matrix led to improvement in the thermal properties of NCs comparing with pure PI. The polymer also gradually changed to an antibacterial agent with the addition of Ag NPs into a PI matrix.

REFERENCES

1. Singh, G.; Patankar, R. B.; Gupta, V. K. *Polym. Plast. Technol. Eng.* **2010**, *49*, 1329.
2. Zhu, A.; Cai, A.; Zhang, J.; Jia, H.; Wang, J. *J. Appl. Polym. Sci.* **2008**, *108*, 2189.
3. Ganeev, R. A.; Baba, M.; Ryasnyansky, A. I.; Suzuki, M.; Kuroda, H. *Opt. Commun.* **2004**, *240*, 437.
4. Gan, X.; Liu, T.; Zhong, J.; Liu, X.; Li, G. *ChemBioChem* **2004**, *5*, 1686.
5. Son, W. K.; Youk, J. H.; Lee, T. S.; Park, W. H. *Macromol. Rapid Commun.* **2004**, *25*, 1632.
6. Karthikeyan, B. *Phys. B: Condens. Matter* **2005**, *364*, 328.
7. Dubas, S. T.; Pimpan, V. *Mater. Lett.* **2008**, *62*, 3361.
8. Yeum, J. H.; Sun, Q.; Deng, Y. *Macromol. Mater. Eng.* **2005**, *290*, 78.
9. Sroog, C. E. *Prog. Polym. Sci.* **1991**, *16*, 561.
10. Liaw, D. J.; Wang, K. L.; Huang, Y. C.; Lee, K. R.; Lai, J. Y.; Ha, C. S. *Prog. Polym. Sci.* **2012**, *37*, 907.
11. de Abajo, J.; de la Campa, J. G. In Progress in Polyimide Chemistry I; Kricheldorf, H. R., Ed.; Springer: Berlin/Heidelberg, **1999**, Chapter 2.
12. Dhara, M. G.; Banerjee, S. *Prog. Polym. Sci.* **2010**, *35*, 1022.
13. Hajibeygi, M.; Shabanian, M.; Moghanian, H.; Khonakdar, H. A.; Haußler, L. *RSC Adv.* **2015**, *5*, 53726.
14. Zhai, L.; Yang, S.; Fan, L. *Polymer* **2012**, *53*, 3529.
15. Varganici, C. D.; Rosu, D.; Barbu-Mic, C.; Rosu, L.; Popovici, D.; Hulubei, C.; Simionescu, B. C. *J. Analyt. Appl. Pyrol.* **2015**, *113*, 390.
16. Mohanty, A. K.; Misra, M.; Drzal, L. T. *J. Polym. Environ.* **2002**, *10*, 19.
17. Gandini, A. *Macromolecules* **2008**, *41*, 9491.
18. Sheldon, R. A. *Green Chem.* **2014**, *16*, 950.
19. Fache, M.; Darroman, E.; Besse, V.; Auvergne, R.; Caillol, S.; Boutevin, B. *Green Chem.* **2014**, *16*, 1987.
20. Mialon, L.; Pemba, A. G.; Miller, S. A. *Green Chem.* **2010**, *12*, 1704.
21. Peng, H.; Xiong, H.; Li, J.; Xie, M.; Liu, Y.; Bai, C.; Chen, L. *Food Chem.* **2010**, *121*, 23.
22. Fache, M.; Boutevin, B.; Caillol, S. *Eur. Polym. J.* **2015**, *68*, 488.
23. Tamami, B.; Yeganeh, H. *Eur. Polym. J.* **2002**, *38*, 933.
24. Elladiou, M.; Patricklos, C. S. *Polym. Chem.* **2012**, *3*, 3228.
25. Liaw, D. J.; Wang, K. L.; Chang, F. C. *Macromolecules* **2007**, *40*, 3568.
26. Grabiec, E.; Kurcok, M.; Ewa, S. B. *J. Phys. Chem. A* **2009**, *113*, 1481.
27. Wang, K. L.; Liou, W. T.; Liaw, D. J.; Huang, S. T. *Polymer* **2008**, *49*, 1538.
28. Hajipour, A. R.; Zahmatkesh, S.; Banihashemi, A.; Ruoho, A. E. *Polym. Bull.* **2007**, *59*, 145.
29. Weiss, M. *J. Am. Chem. Soc.* **1952**, *74*, 200.
30. Tamami, B.; Yeganeh, H. *Polymer* **2001**, *42*, 415.
31. Weiss, M. *J. Am. Chem. Soc.* **1952**, *74*, 200.
32. Shabanian, M.; Mirzakhanian, Z.; Basaki, N.; Khonakdar, H. A.; Faghihi, K.; Hoshyargar, F.; Wagenknecht, U. *Thermochim. Acta* **2014**, *585*, 63.
33. Shabanian, M.; Basaki, N.; Khonakdar, H. A.; Kianipour, S.; Wagenknecht, U. *Polym. Int.* **2014**, *63*, 1658.
34. Hajibeygi, M.; Shabanian, M. *Chin. J. Polym. Sci.* **2014**, *32*, 758.
35. Liu, X. L.; Wu, D.; Sun, R.; Yu, L. M.; Jiang, J. W.; Sheng, S. R. *J. Fluorine Chem.* **2013**, *154*, 16.
36. Schäfer, A. I.; Akanyeti, I.; Semião, A. J. C. *Adv. Colloid Interface Sci.* **2011**, *164*, 100.
37. Chen, G.; Hu, H.; Wu, T.; Tong, P.; Liu, B.; Zhu, B.; Du, Y. *Food Control* **2014**, *35*, 218.
38. Zhu, B. K.; Xie, S. H.; Xu, Z. K.; Xu, Y. Y. *Compos. Sci. Technol.* **2006**, *66*, 548.
39. Kodjie, S. L.; Li, L.; Li, B.; Cai, W.; Li, C. Y.; Keating, M. *J. Macromol. Sci. B* **2006**, *45*, 231.